

## Analysis of the Magnetic Properties of RFe<sub>11</sub>Ti and RFe<sub>11</sub>TiH (R=Tb, Ho)

S. W. Xu<sup>1</sup>, Y. Yan<sup>1,2\*</sup>, H. M. Jin<sup>1</sup>, X. F. Wang<sup>1</sup>, W. Q. Wang<sup>1</sup>, and F. Su<sup>1</sup>

<sup>1</sup>Department of Physics, Jilin University, Changchun 130023, P.R. China

<sup>2</sup>State Key Laboratory for Superhard Materials, Jilin University, Changchun 130023, P.R. China

(Received 8 December 2003)

The values of crystalline-electric-field parameters  $A_{nm}$  for RFe<sub>11</sub>TiH<sub>x</sub> (R=Tb, Ho) (x=0,1) are obtained by fitting calculations to the magnetization curves along the crystal axes at 4.2 K and higher temperatures. The insertion of H element in RFe<sub>11</sub>Ti significantly affects CEF parameters  $A_{nm}$ . By using exchange field  $2\mu_B H_{ex}$  derived by inelastic neutron scattering and fitted  $A_{nm}$ , the calculations reproduce the experimental curves well.

**Key words :** crystalline-electric-field, rare-earth 3d metal compound, magnetization curve

### 1. Introduction

During the last few years, the magnetic properties of the intermetallic compounds RFe<sub>11</sub>Ti and their hydrides RFe<sub>11</sub>TiH have been studied extensively [1-8]. Many experimental investigations of the intrinsic magnetic properties of RFe<sub>11</sub>TiH<sub>x</sub> (x=0,1) single crystals have been reported [1-7]. The insertion of hydrogen element in RFe<sub>11</sub>Ti significantly changes their Curie temperature, saturation magnetization and magnetic anisotropy. Nikitin et al evaluated the values of Ho-Fe exchange field  $2\mu_B H_{ex}$  and crystalline-electric-field (CEF) parameters  $A_{nm}$  in HoFe<sub>11</sub>TiH<sub>x</sub>(x=0,1) by fitting calculations to the magnetization curves along the crystal axes at 4.2 K and concluded that hydrogenation leads to the increase in  $2\mu_B H_{ex}$  of about 10% [1]. Inelastic neutron scattering (INS) experiments on RFe<sub>11</sub>Ti and RFe<sub>11</sub>TiN (R=Gd, Er) show that insertion of N element leads to the decrease in  $2\mu_B H_{ex}$  of about 14% [9]. INS experiments on Gd<sub>2</sub>Fe<sub>17</sub> and Gd<sub>2</sub>Fe<sub>17</sub>M<sub>x</sub> (M: C, N, D (deuterium)) also show that insertion of light interstitial element (C, N, D) reduces the Gd-Fe exchange field at Gd site in Gd<sub>2</sub>Fe<sub>17</sub> [10]. In this connection, the insertion of light interstitial elements leads to the enhancement of Curie temperature and the lattice expansion of the compounds.

This work is to evaluate the values of CEF parameters  $A_{nm}$  of RFe<sub>11</sub>TiH<sub>x</sub> (R=Tb, Ho) (x=0,1) from the experimental magnetization curves at 4.2 K and higher temperatures on

the basis of the single-ion model and analyse the experimental data.

### 2. Method of Analysis

RFe<sub>11</sub>TiH<sub>x</sub> (x=0,1) have a ThMn<sub>12</sub>-type tetragonal structure with space group *I4/mmm*. There is one rare-earth ion site with the point symmetry D<sub>4h</sub>. The Hamiltonian of the rare-earth ion consists of the CEF interaction, the R-Fe exchange interaction and the Zeeman energy, i.e.

$$H = H_{CEF} + 2\mu_B \vec{S} \cdot \vec{H}_{ex} + \mu_B (\vec{L} + 2\vec{S}) \cdot \vec{H}, \quad (1)$$

In the coordinate system with *x* and *z* axes along the [100] and [001] axes, respectively, the CEF interaction can be expressed as

$$H_{CEF} = \sum_{n=2,4,6} A_{n0} \sum_j C_{n0}(\theta_j, \varphi_j) + \sum_{n=4,6} A_{n4} \sum_j (C_{n4}(\theta_j, \varphi_j) + C_{n-4}(\theta_j, \varphi_j)), \quad (2)$$

Here

$$C_{nm}(\theta_j, \varphi_j) = [4\pi / (2n + 1)]^{1/2} Y_{nm}(\theta_j, \varphi_j), \quad (3)$$

$Y_{nm}(\theta_j, \varphi_j)$  are the spherical harmonics,  $\theta_j$  and  $\varphi_j$  are the polar and azimuthal angles of the position vector of *j*th 4f electron. It is assumed that the rare-earth ion is trivalent and  $\vec{H}_{ex}$  is proportional to the magnetic moment of the Fe sublattice  $\vec{M}_{Fe}$ . The matrix elements of Eq. (1)

\*Corresponding author: Tel: +86-0431-8499047,  
e-mail: jhm@mail.jlu.edu.cn

are calculated by using the irreducible-tensor-operator technique. For a given applied field  $\vec{H}$  and a direction of  $\vec{H}_{ex}$ , the eigenvalues  $E_i$  and eigenfunctions  $|n_i\rangle$  ( $i = 1, 2, \dots, 2J+1$ ) are obtained by diagonalizing the  $(2J+1) \times (2J+1)$  matrix. The free energy for RFe<sub>11</sub>TiH<sub>x</sub> ( $x=0,1$ ) is given by

$$F(\vec{H}, \vec{M}_{Fe}, T) = -kT \ln Z + K_1(T) \sin^2 \theta_{Fe} - \vec{M}_{Fe}(T) \cdot \vec{H}, \quad (4)$$

Where

$$Z = \sum_i \exp(-E_i/kT), \quad (5)$$

and  $K_1(T)$  is the magnetocrystalline anisotropy constant of the Fe sublattice.  $M_{Fe}(T/T_C)/M_{Fe}(0)$  and  $K_1(T/T_C)/K_1(0)$  for RFe<sub>11</sub>Ti and RFe<sub>11</sub>TiH are taken to be same as those for LuFe<sub>11</sub>Ti and LuFe<sub>11</sub>TiH, respectively [4]. The value of  $M_{Fe}(0)$  is taken to be 20.1  $\mu_B/f.u.$  for RFe<sub>11</sub>Ti and 20.6  $\mu_B/f.u.$  for RFe<sub>11</sub>TiH, respectively.  $K_1(0)=23.6$  K/f.u. for RFe<sub>11</sub>Ti and  $K_1(0)=26.6$  K/f.u. for RFe<sub>11</sub>TiH is same as that for LuFe<sub>11</sub>Ti and LuFe<sub>11</sub>TiH, respectively [4]. The equilibrium direction of  $\vec{M}_{Fe}$  is determined from minimization of  $F(\vec{H}, \vec{M}_{Fe}, T)$ , and the magnetic moments of the rare-earth ion and of RFe<sub>11</sub>TiH<sub>x</sub> ( $x=0,1$ ) are given by

$$\vec{M}_R = -\mu_B \sum_i \langle n_i | \vec{L} + 2\vec{S} | n_i \rangle \exp(-E_i/kT) / Z, \quad (6)$$

$$\vec{M} = \vec{M}_R + \vec{M}_{Fe}. \quad (7)$$

The value of the exchange field  $2\mu_B H_{ex}$  in RFe<sub>11</sub>TiH<sub>x</sub> (R=Tb, Ho) ( $x=0,1$ ) were estimated as follows. The value of  $2\mu_B H_{ex}(T \approx 20$  K) derived by INS experiment is about 470 K, 343 K and 250 K for SmFe<sub>11</sub>Ti [11], GdFe<sub>11</sub>Ti [9] and ErFe<sub>11</sub>Ti [9]. It is known that the value of  $2\mu_B H_{ex}$  decrease monotonically across the rare-earth series from Pr to Er in many Rare-earth-Fe intermetallic compounds [12, 13]. By extrapolating the value for SmFe<sub>11</sub>Ti, GdFe<sub>11</sub>Ti and ErFe<sub>11</sub>Ti according such a variation in  $2\mu_B H_{ex}$  across the RFe<sub>11</sub>Ti series, the value of  $2\mu_B H_{ex}(T \approx 20$  K) for TbFe<sub>11</sub>Ti and HoFe<sub>11</sub>Ti is estimated to be about 285 K and 260 K, respectively. It is assumed that the decrease of  $2\mu_B H_{ex}$  induced by insertion of N element is about five times of the decrease by insertion of H in RFe<sub>11</sub>Ti as in R<sub>2</sub>Fe<sub>17</sub> compounds [10]. The value of  $2\mu_B H_{ex}(T \approx 20$  K) for TbFe<sub>11</sub>TiH and HoFe<sub>11</sub>TiH is estimated to be about 277 K and 253 K.

The values of CEF parameters  $A_{nm}$  were evaluated by fitting calculations to the magnetization curves at 4.2 K and higher temperatures for the single crystals of RFe<sub>11</sub>TiH<sub>x</sub> (R=Tb, Ho) ( $x=0,1$ ).

### 3. Results and Discussion

Table 1 lists the fitted values of CEF parameters  $A_{nm}$ . It can be seen that the value of  $A_{20}$  of RFe<sub>11</sub>TiH increase about 77%~113% towards negative value compared with that of corresponding RFe<sub>11</sub>Ti. In this connection, a Mössbauer study of <sup>155</sup>Gd in GdFe<sub>11</sub>TiH<sub>x</sub> ( $x=0,1$ ) has shown that hydrogenation leads to about 53% increase of the electric field gradients at Gd ion site, which are proportional to  $A_{20}$  [8]. Hydrogenation has also significant effect on the high-order CEF parameters  $A_{nm}$ . The significant changes of  $A_{nm}$  cause the change of magnetic aniso-

**Table 1.** The fitted values of CEF parameters  $A_{nm}$

	$A_{20}$	$A_{40}$	$A_{44}$	$A_{60}$	$A_{64}$
TbFe <sub>11</sub> Ti	-90 K	-4 K	-100 K	2 K	-87 K
TbFe <sub>11</sub> TiH	-160 K	-110 K	34 K	20 K	-25 K
HoFe <sub>11</sub> Ti	-61 K	-122 K	-176 K	432 K	-13 K
HoFe <sub>11</sub> TiH	-130 K	-85 K	-80 K	62 K	-10 K

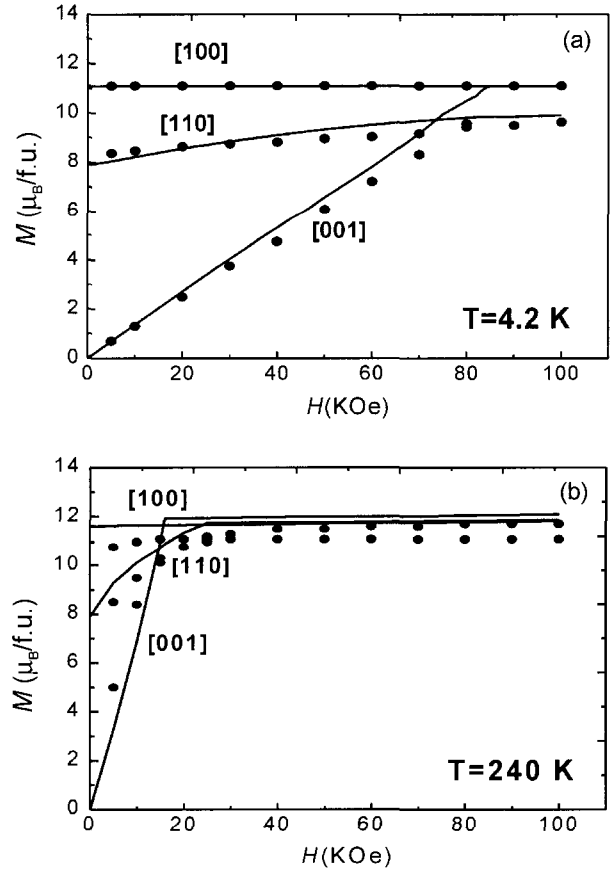


**Fig. 1.** (a) magnetization curves of TbFe<sub>11</sub>Ti at 4.2 K: ● experimental data from [2]; — calculation. (b) magnetization curves of TbFe<sub>11</sub>Ti at 240 K: ● experimental data from [6]; — calculation.

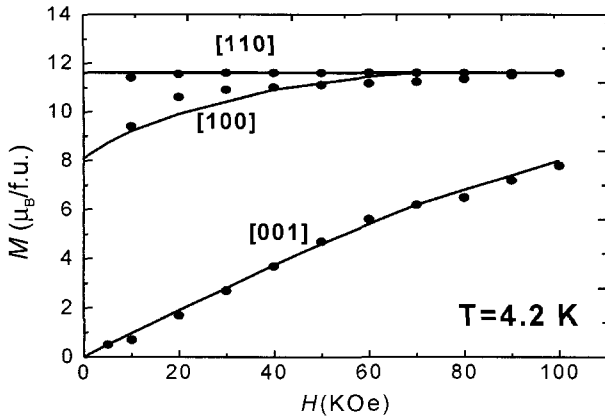


Fig. 2. magnetization curves of  $TbFe_{11}TiH$  at 4.2 K: ● experimental data from [2]; — calculation.

ropy. For example, the change of the easy magnetization direction induced by insertion of H for  $TbFe_{11}Ti$ , which is from the [100] to the [110] axis, mainly originates from a sign change of  $A_{44}$ .

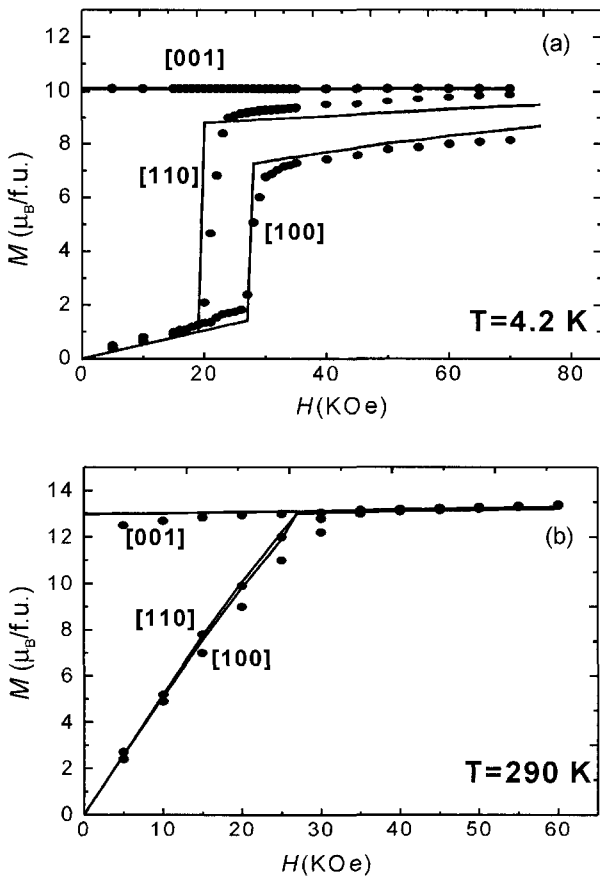


Fig. 3. (a) magnetization curves of  $HoFe_{11}Ti$  at 4.2 K: ● experimental data from [1]; — calculation. (b) magnetization curves of  $HoFe_{11}Ti$  at 290 K: ● experimental data from [6]; — calculation.

Fig. 1 to 4 show the comparison of the calculations with the experimental data. The symbols represent the experimental data, and the full curves the calculations. Fig. 1(a) and 1(b) show the magnetization curves along the [100], [110] and [001] axes at 4.2 K and 240 K for  $TbFe_{11}Ti$ . Fig. 2 shows the magnetization curves along the [100], [110] and [001] axes at 4.2 K for  $TbFe_{11}TiH$ . Fig. 3(a) and 3(b) show the magnetization curves along the [100], [110] and [001] axes at 4.2 K and 290 K for  $HoFe_{11}Ti$ . Fig. 4(a) and 4(b) show the magnetization curves along the [100], [110] and [001] axes at 4.2 K and 300 K for  $HoFe_{11}TiH$ . At 4.2 K, a field-induced first-order magnetization process (FOMP) in the [001] direction was found by our calculation for  $HoFe_{11}TiH$ . It may be as in the FOMP in the  $DyFe_{11}Ti$  [14] that a continuous increase of the magnetization instead of a discontinuous jump in the experimental curves is observed for magnetic field around the critical field. The predicted FOMP by calculation need to be confirmed by the singular-point-detection technique in  $HoFe_{11}TiH$ .

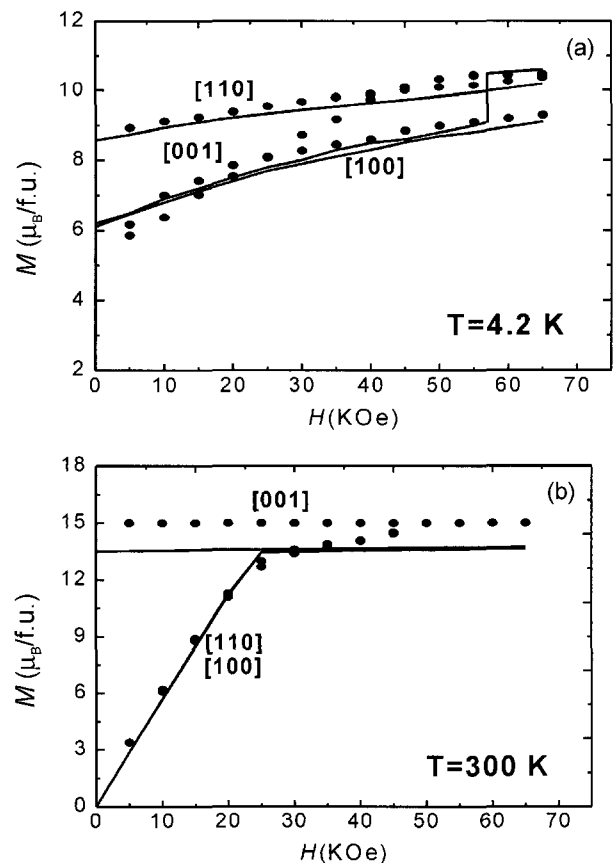


Fig. 4. (a) magnetization curves of  $HoFe_{11}TiH$  at 4.2 K: ● experimental data from [1]; — calculation. (b) magnetization curves of  $HoFe_{11}TiH$  at 300 K: ● experimental data from [7]; — calculation.

## Acknowledgements

This work has been supported by the National Natural Science Foundation of China (Grant No. 10304006) and Specialized Research Fund for Doctoral Program of Higher Education.

## References

- [1] S. A. Nikitin, I. S. Tereshina, N. Yu Pankratov and Yu V Skourski, *Phys. Rev. B* **63**, 35 (2001).
- [2] S. A. Nikitin, I. S. Tereshina, V. N. Verbetsky, A. A. Salamova, and K. P. Skokov, *J. Alloys Comp.* **322**, 42 (2001).
- [3] I. S. Tereshina, P. Gaczynski, V. S. Rusakov, H. Drulis, and S. A. Nikitin, *J. Phys.: Condens. Matter.* **13**, 8161 (2001).
- [4] I. S. Tereshina, S. A. Nikitin, N. Yu Pankratov, G. A. Bezkorovajnyaya, A. A. Salamova, V. N. Verbetsky, T. Mydlarz, and Yu. V. Skourski, *J. Magn. Magn. Mater.* **231**, 213 (2001).
- [5] S. A. Nikitin, I. S. Tereshina, V. N. Verbetsky, and A. A. Salamova, *J. Alloys Comp.* **316**, 46 (2001).
- [6] C. Abadia, P. A. Algarabel, B. Garcia-Landa, M. R. Ibarra, A. del Moral, N. V. Kudrevatykh, and P. E. Markin, *J. Phys.:Condens. Matter.* **10**, 349 (1998).
- [7] S. A. Nikitin, I. S. Tereshina, Yu. V. Skourski, N. Yu Pankratov, K. P. Skokov, V. V. Zubenko, and I. V. Telegina, *Physics of the Solid State* **43**, 290 (2001).
- [8] O. Isnard, P. Vulliet, J. P. Sanchez, and D. Fruchart, *J. Magn. Magn. Mater.* **189**, 47 (1998).
- [9] D. P. F. Hurley, M. Kuzímin, J. M. D. Coey, and M. Kohgi, *J. Magn. Magn. Mater.* **140-144**, 1027 (1995).
- [10] O. Isnard, A. Sippel, M. Loewenhaupt, and R. Bewley, *J. Phys.:Condens. Matter* **13**, 3533 (2001).
- [11] O. Moze, R. Caciuffo, H. S. Li, B. P. Hu, J. M. D. Coey, R. Osborn, and A. D. Taylor, *Phys. Rev. B* **42**, 1940 (1990).
- [12] E. Belorizky, M. A. Fremy, J. P. Gavigan, D. Givord, and H. S. Li, *J. Appl. Phys.* **61**, 3971 (1987).
- [13] M. Loewenhaupt, and I. Sosnowska, *J. Appl. Phys.* **70**, 5967 (1991).
- [14] B. P. Hu, H. S. Li, J. M. D. Coey, and J. P. Gavigan, *J. Phys.: Condens. Matter* **413**, 2221 (1990).